Solute Species Behavior Near a Crystal Surface

Tobias Mazal

ChE 210D

December 11, 2019

Molecular dynamics simulations were conducted to study the interaction between a crystallizing species in solution with a body-centered cubic (bcc) crystal lattice and with solvent molecules. An attractive potential is considered amongst the solute and crystal molecules. We examine the bulk and surface diffusivities at various simulation conditions, and employ umbrella sampling to determine the form of the potential of mean force (PMF).

1 Background

Crystallization is commonly used in industrial processes to convert solute molecules dissolved in solvent to a structured solid state. Pharmaceutical companies often crystallize APIs in the form of organic molecules to selectively formulate specific crystal habits for optimal bioperformance [1]. Crystal engineering is also of importance for developing catalysts with tailored surfaces to maximize active sites or for varying electrical and optical properties in the field of electronic materials such as OLEDs [2, 3]. Given the ubiquity of crystal growth in industrial processes, there is substantial demand for predictive and mechanistic modelling of crystallization. Molecular dynamics may be used to study transport of solute growth units (i.e. atoms, molecules, ions) in crystallization systems. The growth rate of a crystal face is proportional to the rate of growth unit incorporation into kink sites, which is governed by solute diffusion [4]. Thus, we investigate the diffusion of solute growth units both in the bulk solution and on the crystal surface. These solute growth units represent the crystallizing species, but the time scales of crystallization itself are too long to simulate via MD without the use of directed techniques.

2 Simulation Methods

Simulations are conducted in an NVE ensemble after minimizing the energy via a conjugate gradient search and after equilibrating the system via velocity rescaling to a target reduced temperature, T^*. The system is modelled as a number ($N_{solute} = 32$) of solute molecules in a pool of solvent molecules ($N_{solvent} = 544$). The crystal surface is made up of solute molecules ($N_{crystal} = 484$) in a bcc lattice, whose forces and velocities are zeroed. A screenshot of the simulation is given in Figure 1. Periodic boundary conditions are employed through minimum image conventions in the x,y,z directions. Furthermore, a box length of $L = 11$ is selected to screen the finite-size effects. This gives 9 layers of solution and 4 layers of the crystal, which is packed more closely. Data is collected every 500 MD steps during the production run to ensure independent sampling. Interactions amongst species are described through Lennard-Jones (LJ) potentials coupled with harmonic potentials.

$$U^*_{LJ} = \sum_{i<j} 4(r_{ij}^{-12} - r_{ij}^{-6}) \tag{1}$$

$$U^* = \sum_{i<j,unbonded} 4(r_{ij}^{-12} - 2r_{ij}^{-6}) + \sum_{i<j,bonded} \frac{k}{2}(r_{ij} - r_0)^2 \tag{2}$$

Equation 1 is the standard LJ potential, and quantifies the interaction between solvent molecules both with each other and with solute molecules. Equation 2 describes the interactions between solute molecules with

each other in solution and with the same species of molecules found in the crystal layers. This features a modified LJ potential with a stronger attractive term between the crystallizing species, and a harmonic potential to represent the solute molecules as polymers of chain length M. Standard values of $k = 3000$ and $r_0 = 1$ are selected. In order to qualitatively represent stronger attraction between the crystallizing species, we arbitrarily select a prefactor of 2 for the attractive term. In future studies, one could also examine the effect of varying the LJ potentials according to experimentally determined energetic parameters amongst molecules. One may use mixing rules for ϵ and σ parameters to represent interactions amongst distinct species. Note that these equations as well as all reported parameters herein are in reduced units according to the dimensionless form of LJ. Unit masses are used. Furthermore, the LJ potentials are truncated and shifted with $r_c = 2.5$.

Diffusivities are determined from slope of mean squared displacement over time according to Equation 3.

$$D = \lim_{t \to \infty} \frac{\langle |r - r_0|^2 \rangle}{2dt} \tag{3}$$

Here, d corresponds to the dimensionality of the system. For bulk solution diffusivity calculations, we take $d = 3$, as the molecule can travel in the x,y,z dimensions. For the surface diffusivity calculations, we take $d = 2$, as the molecule is constrained from moving in the z direction. Longer equilibration periods are used for calculation of surface diffusivity to ensure that the solute molecules equilibrate on the surface and do not move within the z dimension. Error in diffusivity calculations is given as the standard error in the mean over 5 simulations with different initial random number seeds.

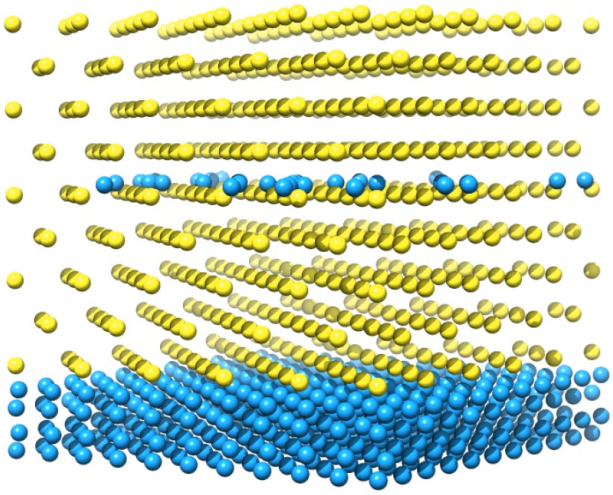

Figure 1: A molecular image of the simulation generated with UCSF Chimera. A box of length $L = 11$ is simulated containing solvent molecules (yellow) and solute molecules (blue). The bcc crystal surface is made up of the same species as the solute molecules (blue).

3 Results and Discussion

3.1 Solute Diffusivity

Diffusivities of the solute molecules are calculated both in the bulk solution and on the (100) face of the bcc crystal surface at various temperatures and polymer chain lengths. For determining the bulk solution diffusivity, simulations underwent a equilibration period of 20,000 MD steps followed by a production run of 100,000 MD steps. The crystal surface is not included in these simulations to ensure bulk diffusivity calculations. The calculated bulk diffusivities are given in Figure 2.

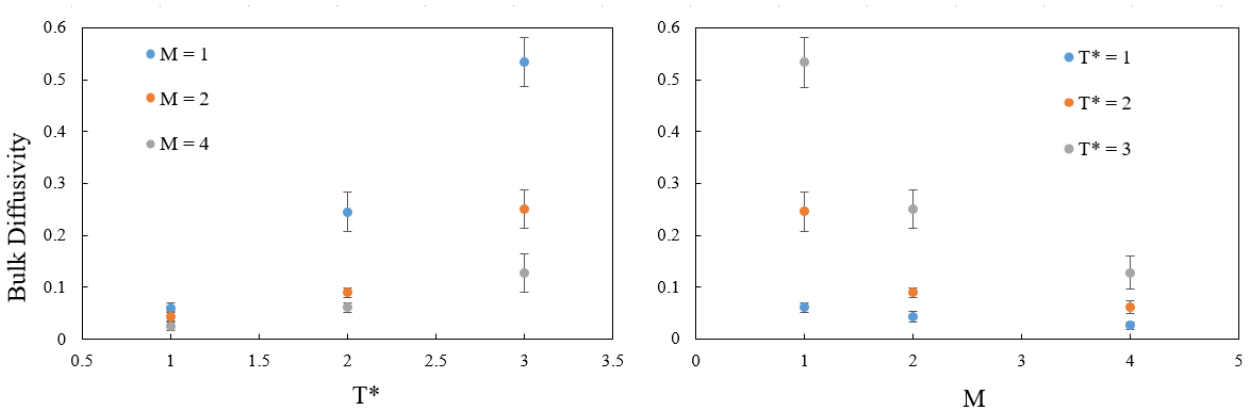

Figure 2: Bulk diffusivity of the solute at various reduced temperatures (T^*) and chain lengths (M). Error bars represent the standard error in the mean over 5 simulations.

We see that increasing the initial reduced temperature results in higher diffusivities, as the particles diffuse faster with higher thermal energy. The relation of diffusivity to temperature may be represented through expressions such as the Arrhenius equation, which may be used to give an "activation energy" for diffusion. We see that at higher chain lengths, the diffusivity decreases for larger and heavier polymers. This trend may also be quantified through scaling laws such as D $\sim M^{\nu}$. More conditions may be probed in future work to better elucidate the scaling of diffusivity with these parameters.

We also calculate the diffusivities on the crystal surface. In this case, the simulations underwent an equilibration period of 100,000 MD steps, and a production run of 200,000 MD steps. Solute positions were checked after the equilibration period to ensure they were "adhered" to the crystal surface. These simulations were run at lower reduced temperatures to prevent thermal fluctuations from knocking the adhered molecules from the surface. The calculated surface diffusivities are given in Figure 3.

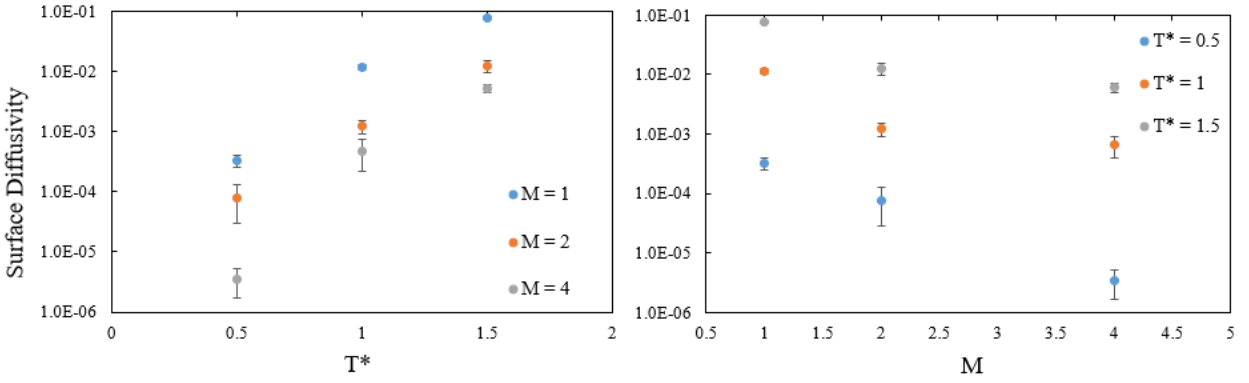

Figure 3: Surface diffusivity of the solute at various reduced temperatures (T^*) and chain lengths (M). Error bars represent the standard error in the mean over 5 simulations. Note the logarithmic scaling of the diffusivities in these graphs.

We observe comparable effects of reduced temperature and chain length on the surface diffusivity as seen in Figure 2. Again, higher temperature increases the diffusion of solute molecules upon the surface, and longer polymers experience larger barriers to diffusion. While we may observe similar trends, the surface diffusivities calculated are orders of magnitude lower than the bulk values, as shown by the logarithmic y-axis. This is due to the strong solute species attraction to the crystal molecules, effectively binding them to the surface.

3.2 Umbrella Sampling

Free energy calculations are useful in providing energetic information such as activation energy barriers and free energies of binding. These may be used in calculations of the growth rate of a crystal face, for example. To probe these free energies, we may take advantage of biased ensembles to achieve broader sampling of configurations that are less often visited. In this case, the equilibrium position of solute molecules was near the surface due to the stronger attractive interaction potentials. It is thus harder to sample configuration states further away from the surface. We identify the reaction coordinate for the potential of mean force as the height (z) from the crystal surface. We look to employ umbrella sampling via a harmonic potential, given in Equation 4, to constrain the system into sampling a smaller range of z values [5]. This bias is applied solely to the solute molecules, giving them the potential as seen in Equation 5.

$$\eta_j(z) = -\beta \frac{k_{bias}}{2}(z - z_j)^2 \tag{4}$$

$$U_j^w(r^N) = U^* + \frac{k_{bias}}{2}(z - z_j)^2 \tag{5}$$

$$F(z) = -k_B T \ln(\mathcal{P}_j^w(z)) + k_B T \eta_j(z) + \text{const} \tag{6}$$

After determining an appropriate bias, we apply it to the simulation to calculate the potential of mean force according to Equation 6. The weighted ensemble distribution,$(\mathcal{P}_j^w(z))$, is determined by binning the counts of z observations in each j simulation. The parameter value $k_{bias} = 12$ was selected to sufficiently bias the simulation without narrowing the distribution excessively. 15 simulations were conducted; corresponding z_j were chosen at various spacings to span the range of the simulation box. Simulations were run at $M = 1$, $T^* = 1$, and a diminished box length of $L = 7$ for faster simulations, though production runs still ran for 200,000 MD steps. A single solute molecule in vapor (solventless) is considered.

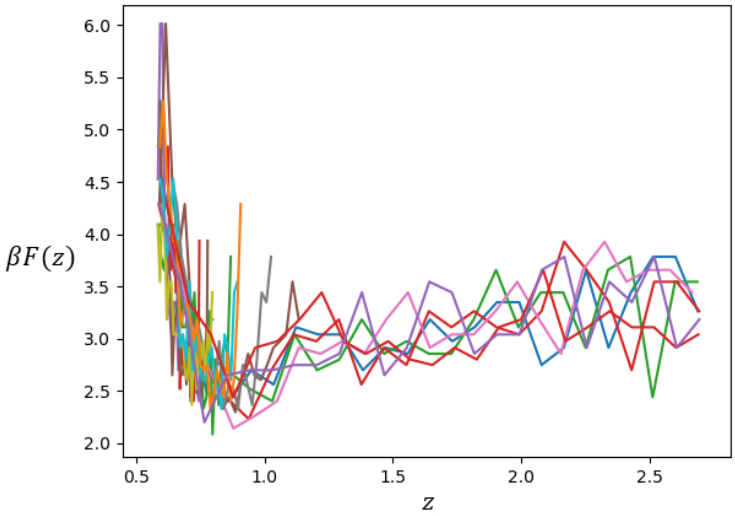

Figure 4: Potential of mean force as a function of reaction coordinate, z.

Figure 4 gives the results of umbrella sampling our system over 15 simulations to determine the potential of mean force. The data is noisy, but one can make out the general form of the potential. This includes an energy well at $z \sim 0.9$ corresponding to the equilibrium position of the solute molecules attracted to the crystal surface. One may dimensionalize the coordinates to see how well the selected potential agrees with lattice parameters for a bcc crystal. At lower z values, there is a high potential of mean force corresponding to the repulsive forces amongst molecules, while the potential levels out to a constant at higher z values.

We ultimately find diffusivities of solute species in bulk and on the (100) bcc crystal surface. These can be used to inform the transport of growth units when considering the growth of a crystal face. Using experimentally determined energetic parameters and mixing rules would enable this approach to yield meaningful data for real systems. However, the generality of these simulations allows for application to a wide range of real crystal systems. Furthermore, histogram techniques can be used to stitch together the curves in Figure 4 and give the underlying potential of mean force to determine free energy differences. In particular, the multiple histogram reweighting method (WHAM) determines the underlying free energy function via maximum likelihood arguments. This would give valuable insight into quantifying free energies of binding and activation energy barriers for incorporation of growth units on a crystal surface. In the future, we may also look to model higher solute concentrations to match supersaturations representative of crystallization systems in practice.

Movie Caption

A movie was created using UCSF Chimera. A box of length $L = 11$ is simulated containing solvent molecules (yellow) and solute molecules (blue). The bcc crystal surface is made up of the same species as the solute molecules (blue). Simulation conditions are $M = 2$ corresponding to dimers in solution, and the reduced temperature is initialized as $T^* = 1$. The first few seconds show equilibration of the system. We see the solute molecules come together as they are more attracted to each other and as they form dimers. As time passes, we see the solute molecules settle on the surface and adopt their equilibrium positions.

References

[1] N. Variankaval, A. S. Cote, and M. F. Doherty, "From form to function: Crystallization of active pharmaceutical ingredients," *AIChE Journal*, vol. 54, pp. 1682–1688, July 2008.

[2] J. D. Rimer, A. Chawla, and T. T. Le, "Crystal Engineering for Catalysis," *Annual Review of Chemical and Biomolecular Engineering*, vol. 9, no. 1, pp. 283–309, 2018.

[3] L. Huang, Q. Liao, Q. Shi, H. Fu, J. Ma, and J. Yao, "Rubrene micro-crystals from solution routes: their crystallography, morphology and optical properties," *Journal of Materials Chemistry*, vol. 20, no. 1, pp. 159–166, 2010.

[4] P. G. Vekilov, "What Determines the Rate of Growth of Crystals from Solution?," *Crystal Growth & Design*, vol. 7, pp. 2796–2810, Dec. 2007.

[5] G. Torrie and J. Valleau, "Nonphysical sampling distributions in monte carlo free-energy estimation: Umbrella sampling," *Journal of Computational Physics*, vol. 23, no. 2, pp. 187 – 199, 1977.